

Formalizing, Normalizing, and Splitting the Energy Network Re-Dispatch for Quantum Annealing

LOONG KUAN LEE¹, JOHANNES KNAUTE², FLORIAN GERHARDT², PATRICK VÖLKER², TOMISLAV MARAS², ALEXANDER DOTTERWEICH², NICO PIATKOWSKI¹

¹Fraunhofer IAIS, ME Group, Sankt Augustin, Germany

²PricewaterhouseCoopers GmbH, Actuarial Risk Modelling, Munich, Germany

Corresponding author: Loong Kuan Lee (e-mail: loong.kuan.lee@iais.fraunhofer.de).

ABSTRACT Adiabatic quantum computation (AQC) is a well-established method to approximate the ground state of a quantum system. Actual AQC devices, known as quantum annealers, have certain limitations regarding the choice of target Hamiltonian. Specifically, the target system must arise from a quadratic unconstrained binary optimization (Qubo) problem. As the name suggests, Qubos represent unconstrained problems, and the problem must fit within the dimensionality limits of the hardware solver. However, various approaches exist to decompose large Qubos and encode constraints by penalizing infeasible solutions. Choosing the right penalization and decomposition techniques is problem-specific and cumbersome due to various degrees of freedom. In this work, we investigate these issues in the context of energy network re-dispatch problems. Such problems are paramount for sustainable and cost-effective energy systems and play a crucial role in the transition towards renewable energy sources. Our Qubo instances are derived from open data of the German energy network and our results are compared to baselines from an open-source energy network simulation, thereby fostering reproducibility. Our novel insights regarding the realization of inequality constraints, spatio-temporal state consistency, and problem decomposition highlight the potential of AQC for optimizing complex energy dispatch problems. This provides valuable insights for energy market stakeholders and researchers aiming to improve grid management and reduce carbon emissions.

INDEX TERMS Quantum Optimization, Constraint Encoding, Energy Network, Grid Management

I. INTRODUCTION

The energy re-dispatch problem has gained increased importance with the rising cost of energy production and the retirement of fossil energy sources. As traditional fossil fuel-based power plants are phased out due to environmental regulations and sustainability goals, the energy grid is increasingly relying on renewable energy sources such as wind and solar. While these renewable sources are cleaner, they are also more variable and less predictable, which complicates the task of balancing supply and demand.

Simultaneously, the cost of energy production is rising due to several factors, including higher fuel prices, increased operational costs, and the investment required to integrate renewable energy sources into the grid. This scenario necessitates a more dynamic and cost-effective approach to energy dispatch. Efficient re-dispatch strategies are crucial to minimize production costs while ensuring that the power system remains reliable and stable. This involves optimizing

the output of available generators, considering the variable nature of renewable energy, and managing the constraints of the power grid. By addressing these challenges, the energy re-dispatch process helps in maintaining a balance between economic efficiency and the transition towards a more sustainable energy future.

The resulting mathematical problems from this scenario are hard combinatorial optimization problems. These problems involve numerous variables and constraints, making them highly complex and difficult to solve. Due to the infamous $P \neq NP$ problem, we do not expect that an efficient algorithm exists for solving these problems optimally in polynomial time. As a result, for large-scale problem instances, no efficient solvers currently exist that can provide optimal solutions within a practical timeframe. This computational challenge underscores the need for advanced optimization techniques and heuristic methods to provide approximate solutions that are both feasible and effective

in real-world applications. However, Quantum Computing could be a viable solution, offering the potential to solve these complex optimization problems more efficiently than classical computing methods.

A. PRACTICAL QUANTUM COMPUTING

Let us quickly introduce the basic notion of what can be considered as quantum computation [1]. Today, practical quantum computing (QC) consists of two dominant paradigms: Adiabatic QC and gate-based QC. In both scenarios, a quantum state $|\psi\rangle$ for a system with n qubits is a 2^n dimensional complex vector. In the gate-based framework, a quantum computation is defined as a matrix multiplication $|\psi_{\text{out}}\rangle = C|\psi_{\text{in}}\rangle$, where the C is a $(2^n \times 2^n)$ -dimensional unitary matrix (the circuit), given via a series of inner and outer products of low-dimensional unitary matrices (the gates). The circuit is derived manually or via heuristic search algorithms [2]. In adiabatic quantum computation (AQC)—the framework that we consider in the paper at hand—the result of computation is defined to be the eigenvector $|\phi_{\text{min}}\rangle$ that corresponds to the smallest eigenvalue of some $(2^n \times 2^n)$ -dimensional Hermitian matrix H . In practical AQC, H is further restricted to be a real diagonal matrix whose entries can be written as $H_{i,i} = H(Q)_{i,i} = \mathbf{x}^i \top Q \mathbf{x}^i$ where $\mathbf{x}^i = \text{binary}(i) \in \{0,1\}^n$ is some (arbitrary but fixed) n -bit binary expansion of the unsigned integer i . Here, $Q \in \mathbb{R}^{n \times n}$ is the so-called Qubo (Quadratic Unconstrained Binary Optimization) matrix. By construction, computing $|\psi_{\text{out}}\rangle$ is equivalent to solving

$$\min_{\mathbf{x} \in \{0,1\}^n} \mathbf{x} \top Q \mathbf{x}. \quad (1)$$

Adiabatic quantum algorithms rely on this construction by encoding (sub-)problems as Qubo matrices.

In both paradigms, the output vector is 2^n -dimensional and can thus not be read-out efficiently for non-small n . Instead, the output of a practical quantum computation is a random integer i between 1 and 2^n , which is drawn from the probability mass function $\text{Prob}(i) = |\langle i | \psi_{\text{out}} \rangle|^2 = ||\psi_{\text{out}}\rangle_i|^2$. This sampling step is also known as collapsing the quantum state $|\psi_{\text{out}}\rangle$ to a classical binary state $\text{binary}(i)$.

AQC has been applied to numerous hard combinatorial optimization problems [3], ranging over satisfiability [4], routing problems [5] to machine learning [6].

B. FINDINGS

Our contributions can be summarized as follows:

- We provide a principled formalization of the Re-Dispatch problem in the framework of quadratic unconstrained binary optimization.
- We devise a novel normalized version of the unbalanced penalty method for integrating inequality constraints into any Qubo, by incorporating restrictions of the underlying Taylor expansion.
- We formulate a novel α -Expansion algorithm for optimizing very large Re-Dispatch instances. In particular, we integrate the temporal adjacent state switching

constraint that arises as part of the problem formulation into the splitting procedure and not into the objective function. This allows us to find solutions to problems for which standard splitting techniques fail.

- We explain how open source simbench data can be used to construct Re-Dispatch problem instances.
- Finally, numerical experiments are conducted which confirm our theoretical considerations, and show that our proposed approach allows us to address problem sizes that are otherwise infeasible.

II. RELATED WORK

In recent years, there has been a growing interest in addressing challenges related to economic dispatch and power system optimization [7]. Ciornei et al. [8] provided a comprehensive survey of the literature, summarizing developments in economic dispatch over the past two decades and categorizing the research based on market structures and variable generation sources.

Colucci et al. [9] introduced a novel approach to optimize electricity surplus in transmission networks using quantum annealing. They demonstrated that quantum-classical hybrid solvers outperformed classical methods in terms of solution quality, indicating the potential of quantum computing in addressing power network optimization problems.

Lee et al. [10] addressed the economic load dispatch problem with the Hopfield neural network, introducing methods like slope and bias adjustments to expedite convergence. They also explored adaptive learning rates, comparing their effectiveness with traditional fixed learning rates.

Li et al. [11] proposed a method for incorporating thermal stress constraints into generation scheduling, utilizing Lagrangian relaxation and an improved simulated annealing technique. They explored the economic implications of frequent ramping of low-cost generating units and the impact on turbine rotor lifespan.

Liang et al. [12] tackled the dynamic generation allocation problem using the Hopfield neural network, considering factors like load tracking, ramping response rate limits, and spinning reserve requirements. Their approach involved lambda-iteration for static economic dispatch followed by the Hopfield neural network for dynamic dispatch.

Lin et al. [13] presented an algorithm integrating evolutionary programming, tabu search, and quadratic programming to solve the nonconvex economic dispatch problem. They showed that their approach outperformed previous evolutionary computation methods in addressing this challenging problem.

Linnemann et al. [14] addressed congestion management in the European electricity system, emphasizing the need for optimal Re-Dispatch measures. They described a methodology for identifying such measures based on generation dispatches and transmission networks.

Park et al. [15] explored the application of the Hopfield neural network to economic power dispatch with piecewise quadratic cost functions, providing a more realistic represen-

tation of cost functions. Their approach showed promising results compared to traditional numerical methods.

Su et al. [16] introduced a direct-computation Hopfield method for solving economic dispatch problems of thermal generators. This method employed a linear input-output model for neurons, resulting in efficient and effective solutions without the need for iterative approaches.

Tanjo et al. [17] focused on decentralized electricity management systems based on renewable energy sources. They extended a graph partitioning algorithm to address the transfer of electricity surplus between microgrids, reducing the cost of constructing a resilient microgrid system.

Walsh et al. [18] presented an augmented neural network architecture for the unit commitment problem. Their approach combined discrete and continuous terms, resulting in a more general energy function. This method outperformed traditional Hopfield network methods and compared favorably with Lagrangian relaxation.

Yorino et al. [19] proposed a dynamic economic load dispatch method to address the challenges posed by renewable energy integration. This approach aimed to make efficient use of the ramp-rate capability of existing generators in a future power system with limited load-following capacity.

Knueven et al. [20] provided a comprehensive overview of mixed integer programming formulations for the unit commitment problem in power grid operations, highlighting the practical importance of these formulations and introducing novel UC formulations for improved performance.

Ajagekar et al. [21] presented QC-based solution strategies for large-scale scheduling problems in manufacturing systems. They used quantum annealing and classical optimization techniques to tackle mixed-integer linear and mixed-integer fractional programs, demonstrating the efficiency of their hybrid approaches.

Stollenwerk et al. [22] addressed optimization problems over proper colorings of chordal graphs, focusing on the flight-gate assignment problem. They introduced efficient quantum alternating operator ansatz (QAOA) constructions, demonstrating resource scaling as low-degree polynomials of input parameters.

Nikmehr et al. [23] innovatively formulated a quantum unit commitment model and developed a quantum distributed unit commitment (QDUC) approach to solve large-scale discrete optimization problems. Their results showed the potential of quantum computing in tackling complex power system problems.

These works collectively provide a foundation for addressing economic dispatch and power system optimization challenges, incorporating techniques from quantum computing, neural networks, optimization algorithms, and considerations for the evolving energy landscape. For general information on power generation, control, optimal dispatch, planning and scheduling we refer to [24] and [25].

III. BACKGROUND

We start off with some theoretical background on (A)QC in Section I-A and then move to the Re-Dispatch problem.

A. NOTATION

We denote matrices with bold capital letters (e.g. \mathbf{A}) and vectors with bold lowercase letters (e.g. \mathbf{a}). Furthermore, for a vector $\mathbf{a} \in \mathbb{R}^{k_1 \times k_2 \times \dots \times k_n}$, we allow the indexing of the vector via the notation $\mathbf{a}_{i_1, i_2, \dots, i_n}$ in order to get the $(i_1 \cdot (k_2 \times \dots \times k_n) + i_2 \cdot (k_3 \times \dots \times k_n) + \dots + i_n)$ -th element of \mathbf{a} . On the other hand we define \mathbf{A}_i to be the i -th column in matrix \mathbf{A} . We also define $\text{abs}_{\odot}(\mathbf{x})$ as the element-wise absolute value of some vector \mathbf{x} .

Furthermore, we use the following standard terms of linear algebra. Let $\text{diag}(\mathbf{a})$ the $n \times n$ diagonal matrix with $\mathbf{a} \in \mathbb{R}^n$ as its diagonal. We will also use the notation $\mathbf{a} \oplus \mathbf{b}$ to denote the external direct sum or concatenation of two vectors. Additionally, we define \mathbf{I}_n as the n -dimensional identity matrix, \mathbf{J}_n to be the $n \times n$ all-ones matrix, and $\mathbf{1}_n$ to be the n -dimensional vector consisting only of 1s. On the other hand, \mathbf{U}_n is the $n \times n$ upper shift matrix defined as $[\mathbf{U}_n]_{ij} = \delta(i, j + 1)$. Lastly, we will use $\llbracket \cdot \rrbracket$ to denote the Iverson bracket where for some statement P , $\llbracket P \rrbracket = 1$ if P is true.

B. QUBO CLAMPING

Within part of our construction, we will rely on a procedure called clamping. Given an n -dimensional Qubo with matrix \mathbf{Q} , one may obtain a n' -dimensional Qubo with $n' < n$ in which $n - n'$ binary variables of the original Qubo are fixed to user-defined values. To this end, consider a partition \mathcal{P} of $[n]$ into two disjoint subsets A and B . W.l.o.g., let $\mathbf{x} = (\mathbf{x}_A, \mathbf{x}_B)$. We may then declare the values of \mathbf{x}_B as being constants and rewrite $\mathbf{x}^T \mathbf{Q} \mathbf{x} = \mathbf{x}_A^T \mathbf{Q}^A \mathbf{x}_A + \text{const}_B$ where \mathbf{Q}^A represents an $|A|$ -dimensional Qubo and the constant term depends only on the fixed values of \mathbf{x}_B . To construct \mathbf{Q}^A , consider some \mathbf{Q}_{ab} where $a \in A$ and $b \in B$. When the constant \mathbf{x}_b is 0, we can safely ignore \mathbf{Q}_{ab} . When \mathbf{x}_b is fixed to 1, we add \mathbf{Q}_{ab} to the corresponding diagonal entry \mathbf{Q}_{aa}^A . After this has been done for all $a \in A$, we remove all rows and columns from \mathbf{Q} that correspond to variables in B to obtain the final \mathbf{Q}^A .

C. RE-DISPATCH

Formally, we assume a given number n of controllable resources, each being in one of k states for all T discrete points in time. We denote by \mathbf{Z} the $T \times n$ matrix over $\mathbb{N}_{\leq k} = \{1, \dots, k\}$, encoding a specific configuration over all the controllable resources over time. Running the a -th controllable resource in its i -th state produces power $\mathbf{p}_{a,i} \geq 0$. The power production of resource a at time t is then:

$$[\mathbf{P}(\mathbf{Z})]_{t,a} = \sum_{i=1}^k \delta(\mathbf{Z}_{t,a}, i) \cdot \mathbf{p}_{a,i}, \quad (2)$$

where $\delta(x, y)$ evaluates to 1 iff $x = y$ and 0 otherwise.

Assume that at each timepoint $t \in \mathbb{N}_{\leq T}$, we are given a target amount of power $[\tau]_t$ to be produced in total by all n controllable resources. In order to ensure that the demand in power is met at all timepoints, we constrain the total power produced by all resources to be above the given target:

$$\forall t \in \mathbb{N}_{\leq T} : \sum_{a=1}^n P(\mathbf{Z})_{t,a} \geq [\tau]_t \iff P(\mathbf{Z})\mathbf{1}_n \geq \boldsymbol{\tau} \quad (3)$$

However, we also need to ensure that all L transmission lines in the power network are not overloaded as well. To encode this constraint, assume we are given the sensitivity matrix \mathbf{S} with dimensions $n \times L$. This matrix models the amount of power from each n controllable resource that will flow through each of the L transmission lines. Also assume we have a non-negative $T \times L$ matrix \mathbf{M} that represent the rated maximum load for each transmission line over time. Note that the rated maximum load for a transmission line can change over time due to various factors such as the external temperature at that timepoint [26]. With that, the constraint for not overloading the transmission lines in the power network can be formalized as:

$$P(\mathbf{Z})\mathbf{S} \leq \mathbf{M} \quad (4)$$

The last constraint we need to enforce is that the controllable resources can only switch to adjacent states between any two timepoints:

$$\forall t \in \mathbb{N}_{\leq T-1} : \text{abs}_{\odot}(\mathbf{Z}_t - \mathbf{Z}_{t+1}) \leq \mathbf{1}_n \quad (5)$$

The objective function we will minimize is the overall cost of the configuration \mathbf{Z} . Running the a -th controllable resource at timepoint t in its i -th state incurs some non-negative cost $c_{t,a,i} \geq 0$. The production cost for running the configuration \mathbf{Z} is then:

$$C(\mathbf{Z}) = \sum_{t=1}^T \left(\sum_{a=1}^n \sum_{i=1}^k c_{t,a,i} \cdot \delta(\mathbf{Z}_{t,a}, i) \right) \quad (6)$$

Furthermore, in order to discourage frequent state switching, switching the state of the a -th controllable resource from i to i' incurs switching cost $s_a(i, i')$. That is a total switching cost of

$$W(\mathbf{Z}) = \sum_{t=1}^{T-1} \sum_{a=1}^n s_a(\mathbf{Z}_{t,a}, \mathbf{Z}_{t+1,a}) \quad (7)$$

where typically the switching cost is proportional to the difference in the power produced between the two states:

$$s_a(i, i') = \gamma |p_{a,i} - p_{a,i'}| \quad (8)$$

Therefore, the overall cost of the configuration \mathbf{Z} , $\bar{\mathbf{Z}}$ is:

$$C(\mathbf{Z}) + \lambda W(\mathbf{Z}) \quad (9)$$

where $\lambda > 0$ is a parameter that controls how much we wish to penalize switching the states of the controllable resources.

To summarize, the final compound objective function we wish to minimize is:

$$\min C(\mathbf{Z}) + \lambda W(\mathbf{Z}) \quad (10)$$

$$\text{subject to } P(\mathbf{Z})\mathbf{1}_n \geq \boldsymbol{\tau} \quad (11)$$

$$P(\mathbf{Z})\mathbf{S} \leq \mathbf{M} \quad (12)$$

$$\forall t \in \mathbb{N}_{\leq T-1} : \text{abs}_{\odot}(\mathbf{Z}_t - \mathbf{Z}_{t+1}) \leq \mathbf{1}_n, \quad (13)$$

It should be mentioned that an additional implicit constraint here is the plain integer constraint on the configuration variables \mathbf{Z} .

IV. PROBLEM FORMULATION

In order to solve the problem defined above on AQC hardware, we must first devise its Qubo form Eq. (1). To come up with a proper Qubo formulation, let us first rewrite our problem in terms of binary variables \mathbf{x} that represents a vectorized one-hot encoding of the matrix \mathbf{Z} .

Hence, $x_{t,a,i} = \delta(\mathbf{Z}_{t,a}, i)$ and the power produced by the a -th controllable resource at time t becomes:

$$[P(\mathbf{x})]_{t,a} = \sum_{i=1}^k x_{t,a,i} \cdot p_{a,i}. \quad (14)$$

Let us now discuss the constraints.

A. HARD CONSTRAINTS

Our problem contains a couple of constraints that either cannot be, or we do not wish to be, violated at all cost. For instance, any solution of the optimization problem must not violate the one-hot constraint as violations will produce ill-defined solutions. Another constraint that shall not be violated is the constraint that ensures all controllable resources can only switch to adjacent states between adjacent timepoints. This adjacency constraint encodes a physical limitation on the rate at which the controllable resources can change its power production, and therefore violations will lead to changes in power production that cannot be realized.

1) One-Hot Constraint

Recall that we assume that each of the n controllable resources can be in one of k states. Therefore, by using one-hot encoding, we can represent the entries of the integer matrix \mathbf{Z} as a vector of binary variables \mathbf{x} with a length of $T \times n \times k$. However, not all possible values of \mathbf{x} are a valid solution to the problem. Specifically we require the constraint that $\forall t \in [T], a \in [n]$:

$$\sum_{i=1}^k x_{t,a,i} = 1 \iff (\mathbf{I}_{T \times n} \otimes \mathbf{1}_k^T) \mathbf{x} = \mathbf{1}_{T \times n} \quad (15)$$

This constraint can then be expressed as

$$\mathbf{H}(\mathbf{x}) = \mathbf{1}_{T \times n} \iff \|\mathbf{H}(\mathbf{x}) - \mathbf{1}_{T \times n}\|_2^2 = 0 \quad (16)$$

where $\mathbf{H} := \mathbf{I}_{T \times n} \otimes \mathbf{1}_k^T$. We can then incorporate this constraint in the Qubo formulation using the following Qubo matrix:

$$\mathbf{Q}_{\mathbf{H}} = \mathbf{I}_{T \times n} \otimes [\mathbf{1}_{k \times k} - 2\mathbf{I}_k] \quad (17)$$

2) Adjacent State Switching Constraint

Recall from Eq. (13) that we constrained the solution for all $a \in \mathbb{N}_{\leq n}$ and $t \in \mathbb{N}_{\leq T-1}$:

$$\text{abs}_{\odot}(\mathbf{Z}_t - \mathbf{Z}_{t+1}) \leq \mathbf{1}_n \iff |\mathbf{Z}_{t,a} - \mathbf{Z}_{t+1,a}| \leq 1 \quad (18)$$

Let \mathbf{y}_t and \mathbf{y}_{t+1} be the one-hot binary encoding of integers $\mathbf{Z}_{t,a}$ and $\mathbf{Z}_{t+1,a}$ respectively. Then the objective function that satisfies the constraint in Eq. (18) (i.e. is 0 for solutions that satisfy the constraint) is:

$$\min_{\mathbf{y}_t, \mathbf{y}_{t+1}} \mathbf{y}_t^T \mathbf{A} \mathbf{y}_{t+1}, \quad (19)$$

where:

$$[\mathbf{A}]_{i,i'} = \llbracket |i - i'| > 1 \rrbracket \quad (20)$$

We can then duplicate this constraint to be applied on every pair of \mathbf{y}_t and \mathbf{y}_{t+1} in \mathbf{x} with the Kronecker product $\mathbf{U}_{T \times n} \otimes \mathbf{A}$, leading to the final Qubo matrix over all the binary variables in \mathbf{x} being:

$$\mathbf{Q}_A = \mathbf{U}_{T \times n} \otimes \mathbf{A} \quad (21)$$

Here, $\mathbf{U}_{T \times n}$ is the upper shift matrix as defined in Section III.

B. INEQUALITY CONSTRAINTS

Our problem also contains a couple of inequality constraints that we will encode into Qubos using unbalanced penalization. These inequality can sometimes be violated since solutions that violate these constraints do not result in situations that are impossible to occur in reality and sometimes violating these constraints is unavoidable. For instance, it is possible to overload a transmission line in reality at the cost of increased sagging and degradation of the transmission line. With regards to the power production constraint, it can sometimes be impossible for the resources in the power network to produce the target power required due to various factors such as poor weather affecting solar and wind power generation, or the catastrophic failure of a large number of resources.

A popular method for encoding inequality constraints into Qubos is to use slack variables [27]. However, this approach assumes that both $\mathbf{P}(\mathbf{x})\mathbf{S}$ and \mathbf{M} only contain integer values, which is not the case in our problem.

While it is possible to use slack variables to obtain an approximation of an inequality constraint [9], it can lead to a large amount of slack variables in problems with a large amount of constraints. Specifically, in our problem, we have $(L + 1) \times T$ inequality constraints, where L and T can get pretty large. For example, in the power network we will use later in Section VI, $L = 849$ and T can go as high as 192, leading to $850 \times 192 \times s$ slack variables in total, where s is the number of slack variables to use in order to encode each inequality constraint.

Therefore, in order to avoid the use of slack variables, we will use Unbalanced Penalization [28] for encoding the inequality constraints in Eqs. (11) and (12) as Qubos.

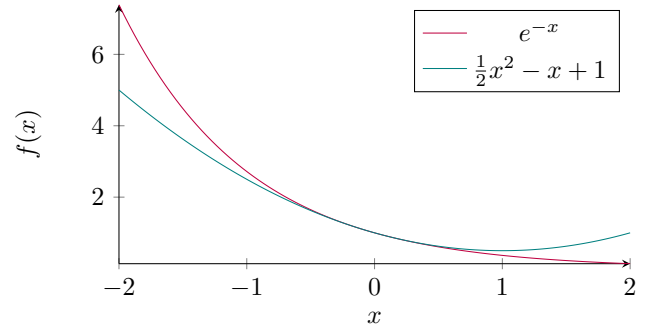


FIGURE 1: Negative exponential and its Taylor approximation to the second order.

To this end, assume we are given constraints in the form:

$$\sum_{i=1}^n l_i \mathbf{x}_i \leq B \iff h(\mathbf{x}) = B - \sum_{i=1}^n l_i \mathbf{x}_i \geq 0. \quad (22)$$

Ideally, we would have a penalty function $P(\mathbf{x})$ (also known as barrier) that significantly penalizes values of \mathbf{x} where $h(\mathbf{x})$ is negative, $h(\mathbf{x}) < 0$. The key idea of unbalanced penalization [28] is to choose the negative exponential function $P(\mathbf{x}) = e^{-h(\mathbf{x})}$ as a barrier. To realize this as a Qubo, P is approximated by the second order Taylor expansion around $h(\mathbf{x}) = 0$. See Figure 1 for an illustration of the difference between e^{-x} and the quadratic approximation of e^{-x} .

$$\begin{aligned} e^{-h(\mathbf{x})} &\approx \zeta(\mathbf{x}) = 1 - h(\mathbf{x}) + \frac{1}{2}h(\mathbf{x})^2 \\ &= 1 - \left(B - \sum_{i=1}^n l_i \mathbf{x}_i \right) + \frac{1}{2} \left(B - \sum_{i=1}^n l_i \mathbf{x}_i \right)^2 \end{aligned} \quad (23)$$

It is important to understand that $e^{-h(\mathbf{x})}$ is only well approximated by the second order Taylor polynomial around $h(\mathbf{x}) = 0$ within the range $h(\mathbf{x}) \in \mathbb{R}_{[-1,1]}$. To enforce a low-approximation error, we propose to normalize the barrier. In fact, we the range of $h(\mathbf{x})$ such that $h(\mathbf{x}) \in \mathbb{R}_{\leq 1}$ since $\forall h(\mathbf{x}) < 0 : \zeta(h(\mathbf{x})) \geq e^{-h(\mathbf{x})}$ and we don't require a good approximation of $e^{-h(\mathbf{x})}$ for negative values of $h(\mathbf{x})$ as long as $\zeta(h(\mathbf{x}))$ is large relative to the expected cost.

Therefore, we derive an upper bound on $h(\mathbf{x})$, $\forall \mathbf{x} : 1/\lceil h \rceil \geq h(\mathbf{x})$, which we utilize for normalization:

$$-\infty < h(\mathbf{x})\lceil h \rceil \leq 1. \quad (24)$$

Clearly, $\lceil h \rceil$ depends on the actual constraint. As we will see in the later subsections, for our constraints, the extrema of $h(\mathbf{x})$ can always be obtained by setting all the resources to their maximum and minimum power production, respectively.

1) Minimum Power Constraint

Recall the constraint on the minimum power to be generated over all resources in Eq. (11):

$$\mathbf{P}(\mathbf{Z})\mathbf{1}_n \geq \tau \quad (25)$$

We can reformulate this constraint in terms of the binary variables leading to T inequalities, $\forall t \in \mathbb{N}_{\leq T}$:

$$\mathbf{g}_t(\mathbf{x}) = \sum_{a=1}^n \sum_{i=1}^k \mathbf{p}_{a,i} \mathbf{x}_{t,a,i} - \tau_t \geq 0 \quad (26)$$

We can then obtain the upper bound on $\mathbf{g}_t(\mathbf{x})$ directly since $\mathbf{g}_t(\mathbf{x})$ is at its maximum when all controllable resources are at their highest power producing state, and the power of all static resources are injected into the power network. Therefore, the upper bound of $\mathbf{g}_t(\mathbf{x})$, $[\mathbf{g}]_t$ is:

$$\frac{1}{[\mathbf{g}]_t} := \max \mathbf{g}_t(\mathbf{x}) = \sum_{a=1}^n \mathbf{p}_{t,a,k} - \tau_t. \quad (27)$$

We now have a vector of upper bounds, and for convenience sake, we also define a vector of the square of these upper bounds:

$$[\mathbf{g}] := \{[\mathbf{g}]_t \mid t \in \mathbb{N}_{\leq T}\} \quad (28)$$

$$[\mathbf{g}^2] := \{[\mathbf{g}^2]_t \mid t \in \mathbb{N}_{\leq T}\} \quad (29)$$

Finally, using unbalanced penalization with this normalizing constant, we have the following objective function for the constraint:

$$\sum_{t=1}^T \left(1 - \mathbf{g}_t(\mathbf{x}) [\mathbf{g}]_t + \frac{1}{2} [\mathbf{g}_t(\mathbf{x}) [\mathbf{g}]_t]^2 \right) \quad (30)$$

which can be encoded as the following Qubo matrix:

$$\mathbf{Q}_g := \frac{1}{2} \bigoplus_{t=1}^T [\mathbf{g}]_t^2 (\mathbf{p}\mathbf{p}^\top) - \text{diag}(\boldsymbol{\zeta} \otimes \mathbf{p}) + (\mathbf{1}_T + \tau \odot \boldsymbol{\zeta}) \otimes (\mathbf{I}_{nk}/n) \quad (31)$$

where:

$$\boldsymbol{\zeta} = [\mathbf{g}] + \frac{1}{2} \tau \odot [\mathbf{g}^2] \quad (32)$$

2) Maximum Line Load Constraint

Let us recall and reformulate the constraint in Eq. (12) in terms of the binary variables \mathbf{x} :

$$\mathbf{P}(\mathbf{x})\tilde{\mathbf{S}} \leq \mathbf{M} \quad (33)$$

Therefore in Eq. (33), we have $L \times T$ inequalities, $\forall l \in \mathbb{N}_{\leq L}, t \in \mathbb{N}_{\leq T}$:

$$\mathbf{h}_{t,l}(\mathbf{x}) = \mathbf{M}_{t,l} - \sum_{a=1}^n \sum_{i=1}^k \mathbf{p}_{a,i} \mathbf{x}_{t,a,i} \mathbf{S}_{a,l} \geq 0 \quad (34)$$

Similar to Section IV-B1, before encoding these inequality constraints as a Qubo matrix, we need to find the maximum value of $\mathbf{h}_{t,l}(\mathbf{x})$ to normalize $\mathbf{h}_{t,l}(\mathbf{x})$ such that its within the

range $\mathbb{R}_{\leq 1}$. We can do this by setting all the resources to their minimum power generation state:

$$\frac{1}{[\mathbf{h}]_{t,l}} := \max \mathbf{h}_{t,l}(\mathbf{x}) = \mathbf{M}_{t,l} - \sum_{a=1}^n \mathbf{p}_{a,1} \quad (35)$$

$$[\mathbf{h}] := \{[\mathbf{h}]_{t,l} \mid t \in \mathbb{N}_{\leq T}, l \in \mathbb{N}_{\leq L}\} \quad (36)$$

$$[\mathbf{h}^2] := \{[\mathbf{h}^2]_{t,l} \mid t \in \mathbb{N}_{\leq T}, l \in \mathbb{N}_{\leq L}\} \quad (37)$$

The approximate objective function for the constraint using unbalanced penalization is then:

$$\sum_{t=1}^T \left(1 - \mathbf{h}_t(\mathbf{x}) [\mathbf{h}]_t + \frac{1}{2} [\mathbf{h}_t(\mathbf{x}) [\mathbf{h}]_t]^2 \right) \quad (38)$$

which can be formulated as the following Qubo:

$$\mathbf{Q}_h = \bigoplus_{t=1}^T \left([\mathbf{S} \text{diag}([\mathbf{h}^2]_t) \mathbf{S}^\top] \otimes \mathbf{1}_{k,k} \right) \odot (\mathbf{p}\mathbf{p}^\top) - \text{diag}(\boldsymbol{\xi} \mathbf{S}^\top \otimes \mathbf{1}_k \odot \mathbf{1}_T \otimes \mathbf{p}) + (\mathbf{M} \odot \boldsymbol{\xi} + \mathbf{1}_{T,L}) \mathbf{1}_L \otimes (\mathbf{I}_{nk}/n) \quad (39)$$

where

$$\boldsymbol{\xi} := \frac{1}{2} \mathbf{M} \odot [\mathbf{h}^2] - [\mathbf{h}]$$

C. OBJECTIVE FUNCTION: PRODUCTION AND SWITCHING COST

Qubo formulations of the constraints are now available. The final missing piece is the Qubo for the production and switching cost. A reformulation of Eq. (6) gives the production cost of a configuration \mathbf{Z} in terms of the binary variables \mathbf{x} :

$$\mathbf{C}(\mathbf{x}) = \sum_{t=1}^T \left(\sum_{a=1}^n \sum_{i=1}^k \mathbf{c}_{t,a,i} \mathbf{x}_{t,a,i} \right) = \mathbf{x}^\top \text{diag}(\mathbf{c}) \mathbf{x} \quad (40)$$

$$\implies \mathbf{Q}_C = \text{diag}(\mathbf{c}) \quad (41)$$

Reformulating the switching cost is slightly more involved. First, we rewrite Eq. (7) in terms of the binary variable \mathbf{x} :

$$\mathbf{W}(\mathbf{x}) = \sum_{t=1}^{T-1} \sum_{a=1}^n \left| \sum_{i=1}^k \mathbf{p}_{t,a,i} \mathbf{x}_{t,a,i} - \sum_{i=1}^k \mathbf{p}_{t+1,a,i} \mathbf{x}_{t+1,a,i} \right| = \sum_{t=1}^{T-1} \sum_{a=1}^n \sum_{i=1}^k \sum_{i'=1}^k \mathbf{x}_{t,a,i} \mathbf{x}_{t+1,a,i'} |\mathbf{p}_{t,a,i} - \mathbf{p}_{t+1,a,i'}| \quad (42)$$

From the latter equation, we can readily read of the quadratic terms:

$$[\mathbf{Q}_W]_{(t,a,i),(t+1,a,i')} = |\mathbf{p}_{t,a,i} - \mathbf{p}_{t+1,a,i'}| \quad (43)$$

Therefore, the final Qubo of our Re-Dispatch problem is:

$$\arg \min_{\mathbf{x} \in \{0,1\}^{k \times n \times T}} \mathbf{x}^\top \mathbf{Q} \mathbf{x} + \mathbf{x}^\top (\mathbf{Q}_H + \mathbf{Q}_A) \mathbf{x} \quad (44)$$

where $\mathbf{Q} = \lambda_g \mathbf{Q}_g + \lambda_h \mathbf{Q}_h + \lambda_C \mathbf{Q}_C + \lambda_W \mathbf{Q}_W$.

While we have shown how each part of the problem can be encoded as a Qubo, it turns out that the resulting matrix \mathbf{Q}

can become rather large: In realistic setups with 5 states per controllable resource and 192 time points, the sheer size of Q exceeds 800 GiB when using double precision arithmetic. Moreover, state-of-the-art quantum annealers have limits on the maximum size of the problem it can solve. We address these issues in the following section.

V. HANDLING HARD CONSTRAINTS VIA α -EXPANSION

The Qubo problems from the previous section can become quite large for realistic setups. Therefore, we need to use decomposers in order to split our problem into a set of smaller instances whose solutions can then be combined to a global solution of the original problem. Various approaches for decomposing Qubos are known and a full review of this topic is out of the scope of this work. We instead focus on an algorithmic approach called α -expansion. Nevertheless, we conduct a comparison of our proposal with four baseline decomposers in Section VII-C.

The core idea of α -expansion is to consider an initial solution \mathbf{x}_0 , that is iteratively refined by selecting a permutation that exchanges the positions of 0s and 1s. At each iteration, we consider a subset of “valid” permutation matrices of \mathbf{x} , $\{\mathbf{C}_1, \dots, \mathbf{C}_c\} \subseteq \mathbb{C}$ —where \mathbb{C} depends on the problem—to apply on the current solution $\hat{\mathbf{x}}$. based in this intuition, a new Qubo can be derived that, instead of directly optimizing the decision variables, optimizes over the choice of $c \in \mathbb{N}$ permutation matrices that are applied to the initial solution as follows [29]:

$$\min_{\alpha \in \{0,1\}^c} \alpha^\top \mathbf{B} \alpha \quad (45)$$

where:

$$E(\mathbf{v}, \mathbf{u}) := \mathbf{v}^\top \mathbf{Q} \mathbf{u} \quad (46)$$

$$\mathbf{c}_i^* := (\mathbf{C}_i - \mathbf{I}_{T \times m \times k}) \mathbf{x} \quad (47)$$

$$[\mathbf{B}]_{i,j} = \begin{cases} E(\mathbf{c}_i^*, \mathbf{c}_j^*) & i \neq j \\ E(\mathbf{c}_i^*, \mathbf{c}_j^*) + E(\mathbf{c}_i^*, \mathbf{x}) + E(\mathbf{x}, \mathbf{c}_j^*) & \text{else} \end{cases} \quad (48)$$

The question now is what should the set of “valid” permutation matrices \mathbb{C} be? Previous literature has shown that the one-hot constraint can be obeyed by limiting \mathbb{C} to just cycles that swap the values between two binary variables that are of the same one-hot encoding [29], [30]. In our problem, these cycles represent changing the state of controllable resource a at timepoint t from state i to i' :

$$F_{t,b,i}(i') := \bigoplus_{(t',a')=(1,1)}^{(T,n)} \begin{cases} \mathbf{R}_k(i, i') & t = t', a = a' \\ \mathbf{I}_k & \text{else} \end{cases} \quad (49)$$

where the matrix $\mathbf{R}_k(i, i')$ is defined as:

$$[\mathbf{R}_k(i, i')]_{i,i'} = [\mathbf{R}_k(i, i')]_{i',i} = 1 \quad (50)$$

$$\text{and } \forall j \in \mathbb{N}_{\leq k} \setminus \{i, i'\} : [\mathbf{R}_k(i, i')]_{j,j} = 1 \quad (51)$$

Algorithm 1: Rectify Non-Adjacent Swaps.

Input: Current Solution — \mathbf{Z} , New State — (t, j, i)

Output: Cycles to Rectify Non-Adjacent Swaps — \mathbf{C}

```

1  $c \leftarrow \mathbf{Z}_{t,j}$ 
2  $\mathbf{C} \leftarrow F_{t,j,c}(i)$ 
3  $l \leftarrow t - 1$ 
4 while  $|c - \mathbf{Z}_{l,j}| > 1$  and  $l \geq 1$  do
5    $c \leftarrow \mathbf{Z}_{l,j}$ 
6    $c^* \leftarrow c - \llbracket \mathbf{Z}_{l,j} < c \rrbracket + \llbracket \mathbf{Z}_{l,j} \geq c \rrbracket$ 
7    $\mathbf{C} \leftarrow F_{l,a,c}(c^*) \mathbf{C}$ 
8    $l \leftarrow l - 1$ 
9  $c \leftarrow \mathbf{Z}_{t,j}$ 
10  $r \leftarrow t + 1$ 
11 while  $|c - \mathbf{Z}_{r,j}^*| > 1$  and  $r \leq T$  do
12    $c \leftarrow \mathbf{Z}_{r,j}^*$ 
13    $c^* \leftarrow c - \llbracket \mathbf{Z}_{r,j}^* < c \rrbracket + \llbracket \mathbf{Z}_{r,j}^* \geq c \rrbracket$ 
14    $\mathbf{C} \leftarrow F_{r,a}(c, c^*) \mathbf{C}$ 
15    $r \leftarrow r + 1$ 
16 return  $\mathbf{C}$ 

```

Moreover, in addition to the plain one-hot constraint from Equation (16), our problem also has the adjacent state constraint in Equation (19). Therefore, finding a suitable \mathbb{C} is a bit more involved.

Instead of a fixed set of permutation matrices \mathbb{C} to iterate over, we will instead iterate over the set of possible states for each controllable resource at each timepoint:

$$\mathbb{S} = \left\{ (t, j, i) \mid \forall t \in \mathbb{N}_{\leq T}, j \in \mathbb{N}_{\leq n}, i \in \mathbb{N}_{\leq k} \right\} \quad (52)$$

Then, given a target state change $S = (t, j, i') \in \mathbb{S}$, Algorithm 1 will create a permutation matrix on the fly based on what elements in the current solution with the target state changes, $F_{t,j,\hat{\mathbf{z}}_{t,j}}(i') \hat{\mathbf{x}}$, need to be swapped in order to rectify $F_{t,j,\hat{\mathbf{z}}_{t,j}}(i') \hat{\mathbf{x}}$ to be valid.

Note that when selecting a subset of possible state changes $\{S_1, \dots, S_c\} \subset \mathbb{S}$, we need to ensure that the resulting c permutation matrices from the rectifying algorithm in Algorithm 1 are all disjoint between each other. We can ensure this by restricting that any state change selected to be considered at each iteration is at least k timepoints away from each other, where k is the number of states a controllable resource can be in. The final approach to using α -expansion for our Re-Dispatch problem can be found in Algorithm 2.

VI. EXPERIMENTAL SETUP

Our problem formulation is only viable if data is available to instantiate the problem and hence, the Qubo matrices. In order to facilitate usage of our model and reproducibility of our results, we provide a walk through on the basis of freely available data.

A. SIMBENCH DATA

We use the simbench [31] dataset 1-EHV-mixed-0-sw. In this network, there are 338 controllable resources. These

Algorithm 2: Re-Dispatch α -Expansion.

Input: Initial Solution — \hat{x} , number of changes — c
Output: Modified Solution — x

- 1 **repeat**
- 2 **repeat**
- 3 Choose random subset of n states in \mathbb{S} whose rectified cycles (alg. 1) $\{C_1, \dots, C_c\}$ are all disjoint.
- 4 Create subproblem QUBO B with cycles $\{C_1, \dots, C_c\}$ and solution \hat{x}
 $\alpha^* \leftarrow \arg \min_{\alpha} \alpha^T B \alpha$.
- 5 Apply cycles selected by α^* on \hat{x}
- 6 **until** Every state change in \mathbb{S} has been considered at least once;
- 7 **until** Some convergence criteria is met;
- 8 **return** \hat{x}

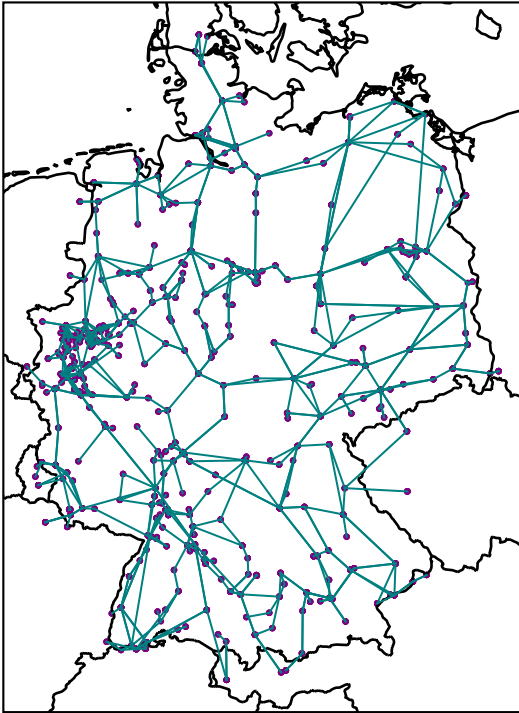


FIGURE 2: Power Network of the Extra High Voltage Grid in the simbench dataset.

controllable resources are of one of the different types listed in Table 1 and have a minimum and maximum production output in Megawatts. The network also has 225 static resources which produces a non-controllable amount of power in Megawatts per timestep. Finally 390 loads and 7 external grid nodes which can either consume power from or inject power into the network. Each of these elements are connected to one of the 3085 substations in the power network. These buses are interconnected by 849 transmission lines, each of

Resource Type	Min Cost	Max Cost
Hard Coal	50	90
Gas	40	100
Solar	30	60
Nuclear	80	120
Offshore wind	70	120
Onshore wind	40	80
Waste	80	110
Lignite	40	70
Oil	90	160
Imported Energy	30	100

TABLE 1: Minimum and maximum cost in € of generating 1 MWh of energy for each type of Controllable Resources based on levelized cost of electricity.

which has a maximum rated current they can transmit. A visualization of this network’s of substations and transmission lines can be found in Fig. 2.

B. EXTRACTING DATA NEEDED FROM SIMBENCH

In order to construct Re-Dispatch problems for the experiments in Section VII, we need to extract the relevant information and data from the simbench dataset. Specifically, we consider data from the first 192 time points of simbench, which represent the data of the network over 2 days. The data from simbench provides the structure and elements of the power network, as well as the power produced or consumed by each element of the power network at each of the 192 timepoints. In the power network of 1-EHV-mixed-0-sw, there are 4 network elements that have an effect on the overall power of the network: controllable resources, static resources, loads on the network, and finally connections to external grids. The sum of the power produced by all of these elements at each timepoint defines the target amount of power we need to produce at each timepoint τ . A power flow simulation via pandapower [32] on the network and data provided by simbench allows us to simulate the amount of power that will flow through each transmission line in the network at each timepoint. With that, we have all the information we need to construct the Re-Dispatch problem described in Section III-C.

In the simbench dataset, each controllable resource has a minimum, $\downarrow \Phi_{\cdot,a}$, and maximum amount, $\uparrow \Phi_{\cdot,a}$, of power it is rated to produce. We then define the discrete power levels the controllable resource can be in via linear steps from $\downarrow \Phi_{\cdot,a}$ to $\uparrow \Phi_{\cdot,a}$, with an additional lowest state of $p_{a,1} = 0$ representing either the a -th controllable resource producing 0 MWh of energy, or the power produced by it not being injected into the power network:

$$p_{a,i} = \begin{cases} \downarrow \Phi_{\cdot,a} + \frac{i-1}{k-1} \cdot (\uparrow \Phi_{\cdot,a} - \downarrow \Phi_{\cdot,a}) & \downarrow \Phi_{\cdot,a} = 0 \\ \downarrow \Phi_{\cdot,a} + \frac{i-2}{k-2} \cdot (\uparrow \Phi_{\cdot,a} - \downarrow \Phi_{\cdot,a}) & \downarrow \Phi_{\cdot,a} \neq 0, i > 1 \\ 0 & \downarrow \Phi_{\cdot,a} \neq 0, i = 1 \end{cases} \quad (53)$$

where k is the desired number of states each controllable resource can be in, and $i \in \mathbb{N}_{\leq k}$.

We assume, the cost of setting the a -th controllable resource to its i -th state can be calculated by multiplying the cost of the resource producing one MWh of energy, c_a^* , with the amount of energy the a -th controllable resource will produce in the i -th state, $p_{a,i}$:

$$\forall t \in \mathbb{N}_{\leq T} : c_{t,a,i} := c_a^* \cdot p_{a,i}. \quad (54)$$

where $a \in \mathbb{N}_{\leq n}, i \in \mathbb{N}_{\leq k}$ and we also assume that the production cost of all controllable resources does not change over time. However, the value of c_a^* depends on the a -th controllable resource's type. Different types of resources will have different ranges in cost for producing one MWh of energy, as we can see in Table 1. For our purposes, we set the value of c_a^* by uniformly sampling between the minimum and maximum cost per MWh, $\downarrow c_a^*$ and $\uparrow c_a^*$ respectively, of the a -th controllable resource's type.

$$c_a^* \sim U(\downarrow c_a^*, \uparrow c_a^*). \quad (55)$$

The next order of business is to find the sensitivity matrix S , which we need to determine how the production of power at some resource affects the amount of power flowing through each transmission line. However, before we do that we need to also record the amount of power produced or consumed by the static resources, loads, and external grids connected to the power network. This results in a matrix where $\hat{\Phi}_{t,c}$ is the amount of power produced or consumed by the c -th element—letting static resource, load, and external grid elements share the same index—where negative values in $\hat{\Phi}$ represents power being consumed by the c -th element. We then estimate the sensitivity matrix using the procedure that us described in Section A of the Appendix with the loss function:

$$\ell(S) = \|\Phi S - \Psi\|_F^2 \quad (56)$$

where:

$$S := \begin{bmatrix} S \\ \hat{S} \end{bmatrix} \quad \Phi = [\Phi \quad \hat{\Phi}] \quad (57)$$

and Ψ is a matrix of the amount of power flow over each transmission line and timepoint.

Finally, we can compute the matrix M where $[M]_{t,l}$ is the maximum load the l -th transmission line can handle at timepoint t . To do so, we first assume that the pair of substations each line is connected to transmits electricity at the same voltage V . Furthermore, from simbench, each transmission line has a maximum rated current it can transmit I . With these simplifications, we arrive at

$$[M]_{t,l} := V \cdot I \cdot \sqrt{3} - [\hat{\Phi} \hat{S}]_{t,l} \quad (58)$$

which is basically the difference between the maximum load the transmission line can carry and the amount of power flowing through the transmission line as a result of the power production and consumption of the static resources, loads, and external grids attached to the network.

Method	Overloaded Lines	Power Fulfill
Baseline	51.5 ±5.41	134% ±1.8%
Ours	9.25 ±1.32	155% ±3.7%

TABLE 2: Comparison of the baseline method for unbalanced penalty and our normalization approach on QUBO $Q_h + Q_g$.

C. RE-DISPATCH PROBLEMS

In order to construct various Re-Dispatch problems from the simbench data, we adjust the number of timepoints in the problem and the number of power levels each controllable resources can be assigned to. Specifically, to limit the number of timepoints in the problem to $T < 192$, we take the data over the 192 timepoints and split them over T equally-sized windows. We then take the mean data over these windows to get T timepoints.

For the experiments in Section VII, we will use the following Re-Dispatch problems of varying sizes:

- (S) 1+2 states (off + min and max output), two time points ($T = 2$)
- (L) 1+4 (off + linear between min and max output) states per controllable, 2 states (on/off) per static, two time points ($T = 8$)

For both setups, we instantiate alle Qubo matrices that appear in our objective function Eq. (44).

VII. RESULTS

Based on our problem setup, we investigate various aspects of our model by conducting four evaluations: First, we study the effectiveness of our novel normalization for the unbalanced penalization. Second, we determine meaningful Lagrange multipliers ($\lambda_g, \lambda_h, \lambda_C, \lambda_W$). Third, we compare our specialized α -expansion to baseline splitting methods. And lastly, we compare the time evolution that is generated by our model to the actual simbench data.

A. UNBALANCED PENALTY: UN-NORMALIZED VS NORMALIZED PENALTY

Recall from Section IV-B that we argued that in order for unbalanced penalization to be theoretically sound, the inequality $h(\mathbf{x}) \geq 0$ needs to be normalized such that $\forall \mathbf{x} : h(\mathbf{x}) \in \mathbb{R}_{(-\inf, 1]}$. In this section we will compare Qubos that encode the inequality constraints in Section IV-B using unbalanced penalization with and without the proposed normalization step in Section IV-B.

Specifically in this experiment, we compare the effectiveness of normalizing $h(\mathbf{x})$ in unbalanced penalization on the S-sized Re-Dispatch problems. We use the S-sized Re-Dispatch problems for this experiment so that we can easily solve the optimization problem without using any decomposition methods—such as α -expansion—whilst ensuring the hard constraints in Section IV-A are not violated. We solve each optimization problem with the classical solver

QUBO	Method	Scores		
		Min	Median	Max
cost (Q_C)	Baseline	0	4.0053×10^7	8.1931×10^7
	Ours	0	0.4889	1
overload (Q_h)	Baseline	849	9.7223×10^2	1.5705×10^3
	Ours	0	0.1708	1
power (Q_g)	Baseline	1	1.7154	3.1341
	Ours	0	0.3352	1
switch (Q_W)	Baseline	0	1.8274×10^4	6.4567×10^4
	Ours	0	0.2830	1

TABLE 3: Distribution of QUBO scores after normalization described in Section VII-B.

TabuSearch from D-Wave’s `dwave-hybrid` package. We then run these experiments over 10 different instantiations, averaging over the 10 different runs and over the 2 timepoints.

In order to study the different approaches to unbalanced penalization, we consider the Qubo $Q_h + Q_g$. Results are shown in Table 2. Compared to the baseline approach, normalization leads to Qubos which are easier to optimize. Keeping all other aspects of the optimization procedure constant, we observe a reduction on the number of overloaded transmission lines, going from an average of 51.5 to 9.25 while the power fulfillment is slightly increased. Note that the power fulfillment is a constraint on the lower limit of produced power. Thus, increasing the production is perfectly fine in the absence of any production cost. Note also that this result is remarkable, since one would expect that an increase in production would imply an increased load on the network. However, our normalization approach allows for a solution that simultaneously improves the satisfiability of both constraints.

B. NORMALIZING QUBO SCORES

Another issue we need to consider is that of finding good Lagrangian multipliers for the Qubos that make up the objective function in Equation (44). However, this can be difficult due to the scale of possible scores, $\mathbf{x}^T Q \mathbf{x}$, for each Qubo can differ massively between each other. Therefore, prior to trying to find values for the Lagrangian multipliers, we follow our approach for the inequality constraints and normalizing the individual Qubos to facilitate equal scaling of all terms involved.

We can normalize each Qubo by using the fact that we know the solutions \mathbf{x} that result in the maximum or minimum score for each Qubo in our objective function. For instance, the cost and overload Qubos return their maximum scores when the solution sets the all the controllable resources to their maximum output value, while their minimum score value is achieved by setting all controllable resources to their minimum values. The opposite is true for the power Qubo. The Qubo responsible for switching costs will be at its maximum score value when the solution constantly switches the states of all controllable resources at every timepoint,

QUBO	Overload (Count)	Cost (€10 ⁶)	Power (Fulfilled %)	Switches (Count)
cost	1	0.0005	0.2693	5.6500
	±0	±0.0008	±0.0004	±9.7136
cost (N)	1	0.0021	0.2700	12.3500
	±0	±0.0032	±0.0016	±13.8385
overload	1	0.0004	0.2692	3.8000
	±0	±0.0007	±0.0003	±6.1653
overload (N)	1	0.0018	0.2698	13.3000
	±0	±0.0024	±0.0010	±11.9355
power	45.40	3.8545	2.2477	63.2000
	±3.45	±0.1082	±0.0479	±4.4360
power (N)	63.75	4.2301	2.4648	59.0500
	±3.48	±0.1080	±0.0296	±5.4235
switch	22.65	2.8517	1.7423	0.4000
	±5.81	±0.1752	±0.1060	±0.3944
switch (N)	27.05	2.8862	1.7612	0.4000
	±4.97	±0.1828	±0.1029	±0.3944

TABLE 4: Statistics and properties of the found minimum solution with and without normalization for each QUBO while optimizing for an objective function containing just that QUBO. QUBOs with normalization are indicated with (N).

while its minimum score state is the solution where no state switching occurs. We then normalize each Qubo Q by subtracting the score of Q with its minimum score value, and dividing by the difference between its maximum and minimum score value:

Let $E_{\min}(Q)$ and $E_{\max}(Q)$ be the minimum and maximum score of Q respectively:

$$E_{\min}(Q) := \min \mathbf{x}^T Q \mathbf{x} \quad (59)$$

$$E_{\max}(Q) := \max \mathbf{x}^T Q \mathbf{x} \quad (60)$$

Then our normalization step involves:

$$\bar{Q} := \frac{Q - \frac{E_{\min}(Q)}{T \times n} \mathbf{I}_{T \times n \times k}}{E_{\max}(Q) - E_{\min}(Q)} \quad (61)$$

$$\implies \mathbf{x}^T \bar{Q} \mathbf{x} = \frac{\mathbf{x}^T Q \mathbf{x} - E_{\min}(Q)}{E_{\max}(Q) - E_{\min}(Q)} \quad (62)$$

since \mathbf{x} is a one-hot encoding of $T \times n$ integers.

We can see from Table 3, that before normalization, the scores $\mathbf{x}^T Q \mathbf{x}$ for the Qubos in the S-sized Re-Dispatch problems differ by 7 orders of magnitude. After normalization on the other hand, the values of $\mathbf{x}^T Q \mathbf{x}$ are within the range $[0, 1]$. We can observe the distribution of these values within $[0, 1]$ in Figure 3.

Similar to Section VII-A, we use 10 different instantiations of the S-sized Re-Dispatch problem for this experiment. We then use TabuSearch to solve an optimization problem that comprises of just one of our 4 Qubos Q_g, Q_h, Q_C, Q_W , each with and without normalization. This results in 8 different optimization problems for each instantiation of the Re-Dispatch problem. Results can be found in Table 4. We can observe that normalizing each Qubos results in qualitative

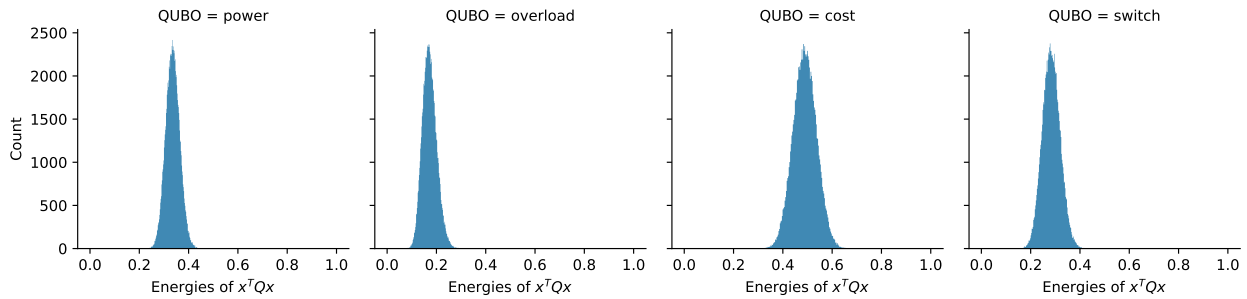


FIGURE 3: Distribution of QUBO Scores $x^T Q x$ in our objective function after normalization.

equivalent solutions. Moreover, due to the aligned scale of our normalized Qubos, we may now express our belief in the importance of each term via intuitive Lagrangian multipliers. In what follows, we chose $\lambda_g = 30$, $\lambda_h = 100$, $\lambda_C = 20$, and $\lambda_W = 0.0001$.

C. DECOMPOSERS

Current day quantum annealers have limits on the maximum size of the problem they can handle. Thus, in case of large problems, we need to use decomposers in order to split our Qubo into a smaller sub-Qubos that can in turn be solved on an actual quantum annealer or a classical solver. D-Wave's `dwave-hybrid` package provides various built-in problem decomposers and in this experiment we compare some of these decomposers to our α -expansion approach as described in Section V.

This comparison is conducted on both S-sized and L-sized Re-Dispatch problems. From Table 5, we can see that for the S-sized problem, the only two decomposers that were able to consistently find solutions that fulfilled the power requirements at each timepoint were α -expansion and `RandomSubproblemDecomposer`. Both these decomposers were also able to carry out an order of magnitude more iterations than the other decomposers. Furthermore, the `RandomSubproblemDecomposer` was able to find a solution with less overloaded power lines than α -expansion, while the latter found solutions with less switches.

On the other hand, for the larger L-sized problem two decomposers did not return a valid solution within the given time. α -expansion outperforms the `RandomSubproblemDecomposer` despite the latter performing more steps than α -expansion. We conjecture that by avoiding solutions that violate the hard constraints in Section IV-A, α -expansion was able to find better solutions to the problem quicker.

D. COMPARISON WITH SIMBENCH DATA

Since our model is instantiated based on the `simbench` data, one may ask how our solution compares to the resource usage of that data. To this end, we run α -expansion with the `TabuSampler` on the L-sized Re-Dispatch for 10 instantiations of the problem. We then compute the time evolution of

(a) S-sized Re-Dispatch Problem with a time limit of 450 seconds

Decomposers (No. Steps)	Overload (Count)	Cost ($\text{€}10^6$)	Power (No. Fulfilled)	Switches (Count)
α -expansion 429.2 \pm 10.2610	11.80 \pm 1.2517	2.5744 \pm 0.0893	2.0 \pm 0.0	64.95 \pm 4.4625
component 23.7 \pm 0.4830	9.20 \pm 1.8288	2.4018 \pm 0.1083	1.7 \pm 0.4830	97.40 \pm 4.0263
roof-dual 840.3 \pm 64.1475	10.25 \pm 1.6202	2.4829 \pm 0.1429	1.9 \pm 0.3162	96.15 \pm 6.3685
score-based 45.3 \pm 0.6749	8.50 \pm 1.4142	2.2384 \pm 0.1602	1.9 \pm 0.3162	95.00 \pm 4.6845
random 755.4 \pm 14.8489	10.45 \pm 1.0659	2.6149 \pm 0.0908	2.0 \pm 0.0	70.60 \pm 6.5141

(b) L-sized Re-Dispatch Problem with a time limit of 900 seconds

Decomposers (No. Steps)	Overload (Count)	Cost ($\text{€}10^6$)	Power (No. Fulfilled)	Switches (Count)
α -expansion 39 \pm 0.8165	3.8375 \pm 0.4861	2.2145 \pm 0.0607	8.0 \pm 0.0	70.3375 \pm 4.0851
component 0.0 \pm 0.0	— —	— —	— —	— —
roof-dual 0.0 \pm 0.0	— —	— —	— —	— —
score-based 4.0 \pm 0.0	11.7625 \pm 1.6345	2.5960 \pm 0.1097	7.9 \pm 0.3162	189.9500 \pm 2.6102
random 192.4 \pm 15.6148	11.4750 \pm 1.7597	2.5811 \pm 0.1056	7.9 \pm 0.3162	190.2000 \pm 2.9990

TABLE 5: Comparison with of α -expansion with various decomposers in D-Wave's `dwave-hybrid` package and the Lagrangian multipliers ($\lambda_g = 30$, $\lambda_h = 100$, $\lambda_C = 20$, $\lambda_W = 0.0001$) on different sizes of the Re-Dispatch problem and different time limits. Dashed entries indicate that the decomposer failed to return a result within the time limit.

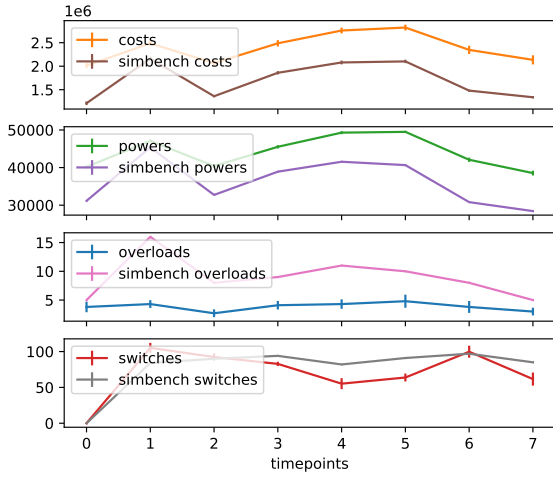


FIGURE 4: Comparison of our configuration with the configuration in the simbench dataset.

cost, power generated, and number of line load violations of the solution and the simbench data.

Results are shown in Fig. 4. First, we see that the estimated cost of our solution are higher. Recall, however, that the cost we assign to each technology are drawn uniformly at random. Hence, this values comes with the largest uncertainty and may change significantly in practice. Remarkably, we find that the solution found by our approach consistently produces more power, while exhibiting far less overloads and less switches than the simbench data.

VIII. CONCLUSION

In conclusion, we proposed a novel, principled formalization of the Re-Dispatch problem in the framework of quadratic unconstrained binary optimization. Due to our generic formalization, this work shall serve as a starting point for other researchers in the field that want to address Re-Dispatch problems via quantum optimization. In order to facilitate a proper realization of inequality constraints as part of the Qubo, we devised a normalized version of the unbalanced penalty method, by incorporating restrictions of the underlying Taylor expansion and problem specific knowledge about configurations that will result in the highest and lowest energy producing states of our objective function (44). An empirical evaluation showed that normalization increases the number of constraints satisfied by the solver. Moreover, we formulated a novel α -Expansion algorithm for optimizing very large Re-Dispatch instances. In particular, we showed how we can specialize α -expansion to not only find solutions that conform to the one-hot constraint in Equation (16), something that has been done before [29], [30], but Re-Dispatch specific constraints, such as the adjacent state switching constraint (19). Finally, we conducted numerical experiments on freely available data. The results confirmed

Algorithm 3: Projected gradient method for estimating sensitivity matrices.

Input: $\tilde{P}, \tilde{\tau}$
Output: S

- 1 $i \leftarrow 0$
- 2 $S^0 \leftarrow I_{m,n}$
- 3 **while not converged do**
- 4 $S^{i+1/2} \leftarrow S^i + \eta^i \nabla \ell(S) + \eta^i \lambda P_{\ell^*, \kappa^*}$
- 5 $S^{i+1} \leftarrow \arg \min_{v \in [0,1]^{m \times n}} \|v - S^{i+1/2}\|_2^2$
- 6 $i \leftarrow i + 1$
- 7 **return** S^i

our theoretical considerations, and show that our splitting approach allows us to address problem sizes that were out of reach for two standard off-the-shelf splitting methods. Finally, the results suggest that our approach was able to find configurations that resulted in less overloaded energy lines and less switches compared to the historical configurations of the same controllable resources in the German energy network found in the simbench dataset.

APPENDIX A ESTIMATING THE SENSITIVITY MATRIX

The sensitivity matrix S encodes how produced energy is distributed over the lines of the network. Here, we explain how S can be obtained from data, e.g., as measured from an actual energy network or obtained from a simulation. The general procedure follows [33]. However, we consider additional regularity constraints. Let $\ell(S) = \|S\tilde{P} - \tilde{\tau}\|_F^2$ denote the loss function of our estimation. \tilde{P} and $\tilde{\tau}$ represent the data: \tilde{P} denotes the produced or consumed energy at the controllable and static resources, $\tilde{\tau}$ represents the recorded or simulated loads on the lines. We estimated S from data by solving the program

$$\min_{S \in [0,1]^{m \times n}} \ell(S) \quad \text{s.t.} \quad \min_{(\ell, \kappa)} (SP)_{\ell, \kappa} \geq 0 \quad (63)$$

via the projected gradient method [34]. The algorithm is provided in Alg. 3.

ACKNOWLEDGMENT

This research has partly been funded by the Federal Ministry of Education and Research of Germany and the state of North-Rhine Westphalia as part of the Lamarr-Institute for Machine Learning and Artificial Intelligence

REFERENCES

- [1] Michael A. Nielsen and Isaac L. Chuang. Quantum Computation and Quantum Information (10th Anniversary edition). Cambridge University Press, 2016.
- [2] Lukas Franken, Bogdan Georgiev, Sascha Mücke, Moritz Wolter, Raoul Heese, Christian Bauchhage, and Nico Piatkowski. Quantum circuit evolution on NISQ devices. In IEEE Congress on Evolutionary Computation (CEC), pages 1–8. IEEE, 2022.
- [3] Andrew Lucas. Ising formulations of many NP problems. Frontiers in Physics, 2, 2014.

- [4] Gary Kochenberger, Fred Glover, Bahram Alidaee, and Karen Lewis. Using the unconstrained quadratic program to model and solve Max 2-SAT problems. *International Journal of Operational Research*, 1(1-2):89–100, 2005.
- [5] Florian Neukart, Gabriele Compostella, Christian Seidel, David von Dollen, Sheir Yarkoni, and Bob Parney. Traffic Flow Optimization Using a Quantum Annealer. *Frontiers in ICT*, 4, 2017.
- [6] Christian Bauchhage, Nico Piatkowski, Rafet Sifa, Dirk Hecker, and Stefan Wrobel. A qubo formulation of the k-medoids problem. In *LWDA*, pages 54–63, 2019.
- [7] Akshay Ajagekar and Fengqi You. Quantum computing for energy systems optimization: Challenges and opportunities. *Energy*, 179:76–89, 2019.
- [8] Irina Ciornei and Elias Kyriakides. Recent methodologies and approaches for the economic dispatch of generation in power systems. *International Transactions on Electrical Energy Systems*, 23(7):1002–1027, 2013.
- [9] Giuseppe Colucci, Stan van der Linde, and Frank Phillipson. Power network optimization: A quantum approach. *IEEE Access*, 11:98926–98938, 2023.
- [10] K.Y. Lee, A. Sode-Yome, and June Ho Park. Adaptive hopfield neural networks for economic load dispatch. *IEEE Transactions on Power Systems*, 13(2):519–526, 1998.
- [11] Zuyi Li and M. Shahidehpour. Generation scheduling with thermal stress constraints. *IEEE Transactions on Power Systems*, 18(4):1402–1409, 2003.
- [12] Ruey-Hsum Liang. A neural-based redispatch approach to dynamic generation allocation. *IEEE Transactions on Power Systems*, 14(4):1388–1393, 1999.
- [13] Whei-Min Lin, Fu-Sheng Cheng, and Ming-Tong Tsay. Nonconvex economic dispatch by integrated artificial intelligence. *IEEE Transactions on Power Systems*, 16(2):307–311, 2001.
- [14] C. Linnemann, D. Echternacht, C. Breuer, and A. Moser. Modeling optimal redispatch for the european transmission grid. In *2011 IEEE Trondheim PowerTech*, pages 1–8, 2011.
- [15] J.H. Park, Y.S. Kim, I.K. Eom, and K.Y. Lee. Economic load dispatch for piecewise quadratic cost function using hopfield neural network. *IEEE Transactions on Power Systems*, 8(3):1030–1038, 1993.
- [16] Ching-Tzong Su and Gwo-Jen Chiou. A fast-computation hopfield method to economic dispatch of power systems. *IEEE Transactions on Power Systems*, 12(4):1759–1764, 1997.
- [17] Tomoya Tanjo, Kazuhiro Minami, and Hiroshi Maruyama. Graph partitioning of power grids considering electricity sharing. *International Journal of Smart Grid and Clean Energy*, 01 2016.
- [18] M.P. Walsh and M.J. O’Malley. Augmented hopfield network for unit commitment and economic dispatch. *IEEE Transactions on Power Systems*, 12(4):1765–1774, 1997.
- [19] Naoto Yorino, Habibuddin M. Hafiz, Yutaka Sasaki, and Yoshifumi Zoka. High-speed real-time dynamic economic load dispatch. *IEEE Transactions on Power Systems*, 27(2):621–630, 2012.
- [20] Bryan Knueven, Jason Ostrowski, and John-Paul Watson. On mixed-integer programming formulations for the unit commitment problem. *INFORMS Journal on Computing*, 32(4):857–876, 2020.
- [21] Anand Ajagekar, Khaled Al Hamoud, and Fengqi You. Hybrid classical-quantum optimization techniques for solving mixed-integer programming problems in production scheduling. *IEEE Transactions on Quantum Engineering*, 3:1–16, 2022.
- [22] Tobias Stollenwerk, Stuart Hadfield, and Zhihui Wang. Toward quantum gate-model heuristics for real-world planning problems. *IEEE Transactions on Quantum Engineering*, 1:1–16, 2020.
- [23] Nima Nikmehr, Ping Zhang, and Maxim A. Bragin. Quantum distributed unit commitment: An application in microgrids. *IEEE Transactions on Power Systems*, 37(5):3592–3603, 2022.
- [24] Allen Wood and Bruce Wollenberg. *Power Generation, Operation, and Control*. John Wiley & Sons, 1996.
- [25] Michael L. Pinedo. *Planning and Scheduling in Manufacturing and Services*. Springer, 2005.
- [26] Soheila Karimi, Petr Musilek, and Andrew M. Knight. Dynamic thermal rating of transmission lines: A review. *Renewable and Sustainable Energy Reviews*, 91:600–612, 2018.
- [27] Fred Glover, Gary Kochenberger, Rick Hennig, and Yu Du. Quantum bridge analytics I: a tutorial on formulating and using QUBO models. *Annals of Operations Research*, 314(1):141–183, July 2022.
- [28] Alejandro Montanez-Barrera, Dennis Willsch, Alberto Maldonado-Romo, and Kristel Michielsen. Unbalanced penalization: A new approach to encode inequality constraints of combinatorial problems for quantum optimization algorithms. arXiv:2211.13914 [quant-ph], June 2023.
- [29] Marcel Seelbach Benkner, Zorah Löhner, Vladislav Golyanik, Christof Wunderlich, Christian Theobalt, and Michael Moeller. Q-Match: Iterative Shape Matching via Quantum Annealing. In *2021 IEEE/CVF International Conference on Computer Vision (ICCV)*, pages 7566–7576, October 2021.
- [30] Thore Gerlach, Stefan Knipp, David Biesner, Stelios Emmanouilidis, Klaus Hauber, and Nico Piatkowski. FPGA-Placement via Quantum Annealing. arXiv:2312.15467 [quant-ph], December 2023.
- [31] simbench. e2nIEEE, March 2024.
- [32] L. Thurner, A. Scheidler, F. Schäfer, J. Menke, J. Dollichon, F. Meier, S. Meinecke, and M. Braun. pandapower — an open-source python tool for convenient modeling, analysis, and optimization of electric power systems. *IEEE Transactions on Power Systems*, 33(6):6510–6521, Nov 2018.
- [33] Ana M. Ospina and Emiliano Dall’Anese. Data-Driven and Online Estimation of Linear Sensitivity Distribution Factors: A Low-rank Approach. arXiv:2006.16346 [math], September 2023.
- [34] Dimitri P. Bertsekas. *Nonlinear Programming*. Athena Scientific, 1999.

...